Time- and spectrally resolved measurements of laser-driven hohlraum radiation

T. Heßling,[1] A. Blažević,[1] A. Frank,[2] D. Kraus,[2] M. Roth,[2] G. Schaumann,[2] D. Schumacher,[2]
T. Stöhlker,[1] and D. H. H. Hoffmann[2]

[1]*GSI Helmholtzzentrum für Schwerionenforschung GmbH, Planckstrasse 1, D-64291 Darmstadt, Germany*
[2]*Institut für Kernphysik, Technische Universität Darmstadt, Schlossgartenstrasse 9, D-64289 Darmstadt, Germany*

(Received 8 November 2010; published 28 July 2011)

At the GSI Helmholtz center for heavy-ion research combined experiments with heavy ions and laser-produced plasmas are investigated. As a preparation to utilize indirectly heated targets, where a converter hohlraum provides thermal radiation to create a more homogeneous plasma, this converter target has to be characterized. In this paper the latest results of these measurements are presented. Small spherical cavities with diameters between 600 and 750 μm were heated with laser energies up to 30 J at 532-nm wavelength. Radiation temperatures could be determined by time-resolved as well as time-integrated diagnostics, and maximum values of up to 35 eV were achieved.

DOI: 10.1103/PhysRevE.84.016412 PACS number(s): 52.38.Ph, 52.40.Mj, 44.40.+a

I. INTRODUCTION

The generation of laser-driven hohlraum radiation and indirect heating of materials with x rays has been widely studied in inertial confinement fusion research over the past decades [1]. For the generation of intense Planck radiation the laser energy is deposited in a converter cavity and multiple absorptions and reemissions transform the x rays into an almost thermal spectral distribution [2]. A large amount of experimental work and theoretical studies have been performed for hohlraum radiation temperatures of several hundred eV, which are necessary for strong radiation shocks [3–5] and fusion [6,7]. Another very interesting application of laser-driven hohlraum radiation is the generation of homogeneous samples of dense plasma by volumetrically heating thin foils with the thermal x rays created in a hohlraum [8]. With this technique dense plasmas with moderate temperatures ($\sim$10 eV) and densities close to solid density can be realized. The understanding of the physics in this parameter region is especially interesting for fusion and astrophysics.

Creating these small samples of dense and relatively cold plasma is, for example, relevant to the measurement of the energy loss of heavy ions in plasma, which is of interest for the fast ignition approach of fusion [9,10]. In these experiments $\sim$500-nm-thick carbon foils are transferred to the plasma state and probed by a conventional accelerator ion beam [11]. Up to now, the heating has been realized by direct laser irradiation, which results in plasma temperatures of more than 100 eV, free electron densities smaller than 10^{21} electrons/cm^3, and strong spatial temperature and density gradients. Indirect heating with hohlraum radiation will give the opportunity to reach the regime of denser and colder plasmas in these experiments. Simulations show that hohlraum radiation temperatures of 30–50 eV are needed to have enough photons at the transparency region near the carbon K edge at 284 eV to transfer the carbon foils into a plasma in the cold and dense parameter regime that does not expand too fast for the diagnostics. For this low-temperature region laser-driven hohlraum radiation has not been well characterized so far and the well-proven scaling laws for higher radiation temperatures have to be validated.

In this paper our latest results of the characterization and performance measurements of the primary converter cavity are presented. Two independent diagnostics have measured the thermal radiation from the hohlraum and a radiation temperature has been deduced.

II. GENERATION OF THERMAL RADIATION

The conversion of coherent laser light into thermal radiation at x-ray wavelengths is, in all its details, a complex process where the material properties of the wall, the laser-plasma interaction, radiation transport, and hydrodynamic motion of the heated wall must be considered. Numerical simulations with appropriate hydrocodes, such as RALEF2D [12] or MIMOZA2D [13], can be used to simulate expected spectra. But, under certain conditions, the underlying physics can be simplified in such a way that the hydrodynamic equations governing the problem exhibit a self-similar solution [14].

When the cold wall is brought into contact with a hot thermal bath (the primary x rays), an ablative heat wave [15] is formed and propagates into the wall. In this overdense region impinging radiation is absorbed, thermalized, and reemitted into the cavity. Considering the energy fluxes from and into a wall element one gets

$$S_s + S_i = S_w + S_r, \tag{1}$$

where S_s are primary x rays, S_i radiation coming from all other wall elements, S_w losses into the wall, and S_r the reemitted flux. In the self-similar case the losses into the wall and the reemitted flux are related to each other:

$$S_r = ct^\alpha S_w^\beta \rightarrow S_r = ct^\alpha (S_s + S_i - S_r)^\beta, \tag{2}$$

with α, β, and c being material constants and t the time. For general geometries the terms S_s and S_i include view factors depending on the relative orientation of any two wall elements to each other. Fortunately, for a spherical cavity, this view factor is a constant and the relation simplifies to

$$S_r = ct^\alpha (S_s - f S_r)^\beta, \tag{3}$$

where f is the ratio of holes to the total inner surface of the sphere. With gold as the wall material one has $c = 4.87$, $\alpha = 8/13$, and $\beta = 16/13$ when the fluxes are expressed in terms of 10^{14} W/cm^2 and the time in nanoseconds. This equation can be used to estimate the achievable radiation temperature

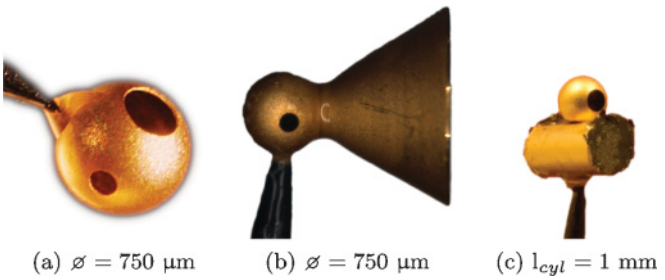

(a) $\varnothing = 750$ µm (b) $\varnothing = 750$ µm (c) $l_{cyl} = 1$ mm

FIG. 1. (Color online) A selection of targets that can be manufactured in our target laboratory: (a) Spherical hohlraum; (b) spherical target with radiation shield; (c) prototype of the interaction target for energy-loss experiments.

in a laser-heated cavity as well as the reemission coefficient (albedo) of the hot inner wall [16]. The assumption of no losses through holes leads to a very simple scaling law for the radiation temperature in a spherical hohlraum with an inner cavity surface A_c heated by a laser with power P_L [1,17]:

$$T_r = 65.2\left[\frac{\eta(P_L/\mathrm{TW})}{(A_c/\mathrm{cm}^2)}(t/\mathrm{ns})^{1/2}\right]^{4/13} \mathrm{eV}. \quad (4)$$

The factor η is the conversion efficiency from laser energy to primary x rays in the hohlraum.

III. TARGET MANUFACTURING

The targets used in the experiments, hollow spheres with diameters of 600–760 μm made of gold, were manufactured at the Technische Universität Darmstadt. In the detector and target laboratory of the nuclear physics institute the production processes to produce many different targets were implemented.

Positive blanks of either brass or steel are at first electroplated with a 10-μm gold layer. A photoresist is deposited onto this and developed at those locations where holes need to be etched into the gold. After etching and cleaning, the different parts of the target are assembled under a microscope. Various types of targets have been produced in such a manner, and some of them are depicted in Fig. 1. The first target is of the type that was used in the experiments with a laser entrance hole diameter of 300 μm and a diagnostic hole of 150 μm. On this target a shielding cone can be directly attached, as shown in Fig. 1(b). Future energy-loss experiments will be carried out with targets of the type depicted in Fig. 1(c). The primary converter is located on top of a secondary cylindrical cavity. The thermal radiation will enter the lower cavity and heat the carbon foils attached on both sides, which are then probed by the heavy-ion beam.

IV. EXPERIMENTAL SETUP

The measurements were performed at the experimental area Z6 of the GSI Helmholtz center for heavy-ion research in Darmstadt, Germany. Here, combined experiments with an ion beam from the UNILAC accelerator and two high-energy laser systems, nhelix [18] and PHELIX [19], are possible. In the experiments presented here the former was utilized as the frequency-doubled beamline of the more energetic PHELIX was not yet available at that time. Gold cavities

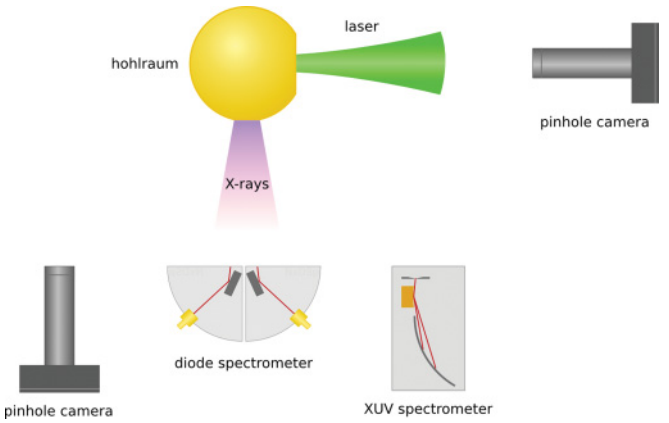

FIG. 2. (Color online) Schematic arrangement of the target and the diagnostics in the experiments. Two temperature diagnostics recorded the thermal radiation while pinhole cameras were used to image the hohlraum.

were heated with pulses of up to 30 J in 7 ns at 532-nm wavelength. An absolutely calibrated diode spectrometer and a time-integrating XUV spectrometer recorded the thermal radiation. A schematic setup is shown in Fig. 2.

The diode spectrometer is a four-channel system where each channel consists of a multilayer x-ray mirror, an x-ray filter to attenuate higher reflection orders, and a silicon diode. Each channel records the absolute radiation power at a different wavelength, so that the brightness temperature of the hohlraum can be deduced for each channel. The brightness temperature is defined as the temperature of a blackbody that emits the same intensity as measured at a given wavelength. For a perfect blackbody the brightness temperature equals the kinetic temperature. The photon energy channels of the time-resolved spectrometer were 180, 280, 450, and 650 eV and were chosen to cover the spectral region around the maximum of the Planck curve. This measurement of the maximum absolute photon flux is of special interest for the future heating of samples by hohlraum radiation. Every single component of the spectrometer was calibrated by its manufacturer; the combined sensitivity of each channel is depicted in Fig. 3. With a time resolution of 1 ns the radiation temperature can be measured during the heating of the cavity.

The radiation intensity of a blackbody spectrum depends on the temperature, the source size, the solid angle, and the wavelength interval that is observed. The solid angle and the wavelength interval are properties of the diagnostic whereas the source size is defined by the size of the diagnostic hole of the targets [see Fig. 1(a)]. Its knowledge is crucial to the analysis and thus each target has to be exactly characterized. Combining the quantum efficiency of each component in a single channel leaves the radiation temperature as the only free parameter. A minimization routine is used to match a measured photocurrent to a theoretical calculated value, and the resulting temperature is defined as the brightness temperature. This analysis is done separately for all four channels, which should yield the same result if the radiation was indeed thermal. Due to the high nonlinearity of the temperature dependence of the radiation power, especially at the maximum of the spectral distribution, all channels exhibit a lower threshold below

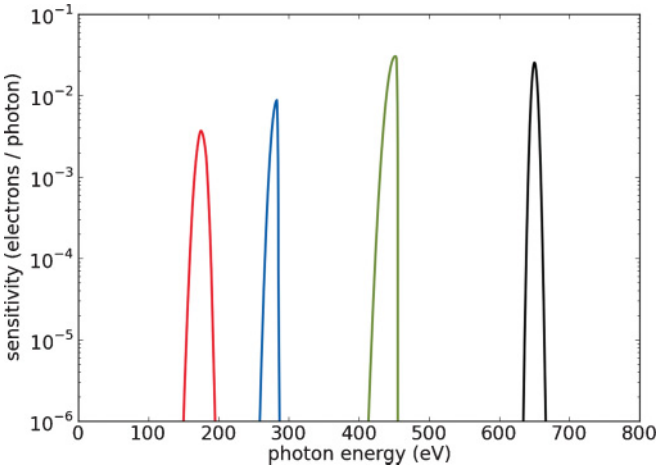

FIG. 3. (Color online) Spectral sensitivity for each of the four channels of the diode spectrometer.

which no temperature can be measured. The noise level of the oscilloscope was ∼1–2 mV, which translates to threshold brightness temperatures of 21 eV up to 24 eV, depending on the channel.

The second, independent diagnostic is a time-integrating grazing incidence spectrometer with a grating of 1200 lines/mm in Rowland geometry. A wavelength interval of 2–50 nm can be observed. Agfa image plates (type MD4.0), together with a Fuji FLA-7000 scanner, were used as a detector. The time integration does not pose a big problem as the power of the thermal radiation rises with the temperature to the fourth power. The maximum temperature during the heating phase will contribute most to the recorded spectrum. So assuming a blackbody and fitting a regular Planck spectrum to the measured one will yield a lower threshold of the maximum temperature as the time integration merely shifts the peak intensity to longer wavelengths. Additionally, one gets information about the agreement of the radiation spectrum with a perfect blackbody spectrum. The sensitivity of the image plates at wavelengths of a few nanometers is unknown and assumed to be constant [20].

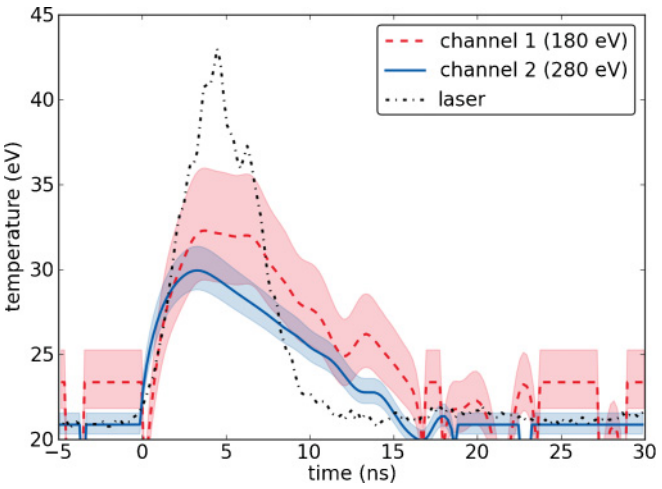

FIG. 4. (Color online) Time-resolved temperature evolution of a hohlraum target heated with 17-J laser energy.

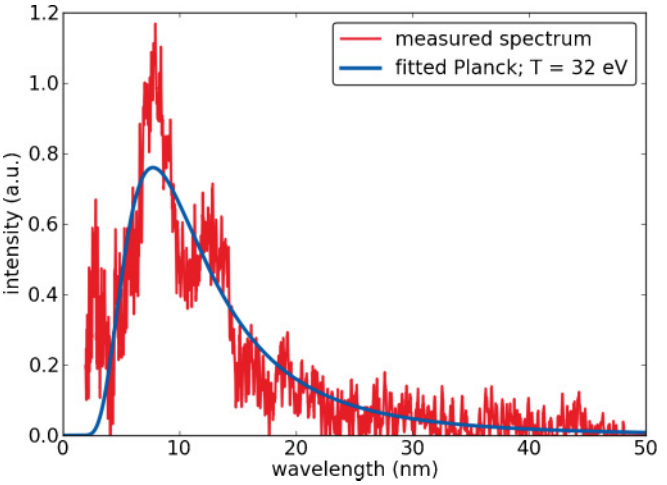

FIG. 5. (Color online) Measured time-integrated spectrum with a fitted Planck spectrum of 32 eV.

V. TIME-RESOLVED MEASUREMENTS

Cavities of different sizes were heated with different energies varying between 15 and 30 J. One of the recorded time-resolved temperature evolutions is shown in Fig. 4. The solid area marks the total error of the system. In this measurement both channels show the same temperature curve within the error margin and reach a maximum value of ∼32 eV. From the temporal laser profile it is obvious that the temperature follows the intensity of the laser. At the end of the heating phase the temperature does not decrease instantly with the laser pulse due to the time it takes the target to cool radiatively.

Time-resolved measurements have the advantage that they directly deliver the maximum radiation temperature. No assumptions on the influence of time integration by regular spectrometers are needed. On the contrary, these assumptions can be verified with such a time-resolving diagnostic, and this will be done in the next section.

VI. TIME-INTEGRATED MEASUREMENTS

Time-integrated spectra of the same targets were recorded with the XUV spectrometer. Since it was not calibrated in intensity, only the spectral distribution of the radiation can be used to retrieve temperature information. A scaled Planck curve was fitted to the measured spectra, and the resulting temperature was defined as the radiation temperature.

A sample measurement of a hohlraum with the same size as before and comparable laser energy as in the time-resolved case is shown in Fig. 5, together with the fitted Planck curve. The temperature of 32 eV fits very well to the maximum temperature from the diode spectrometer. This confirms that the integration indeed has little effect when one is only interested in the maximum temperature, and that the assumption of perfect blackbody radiation can be used reasonably well. But time information is valuable, for example, as input to hydrodynamical simulations, as well as calculating the amount of energy transferred into thermal radiation.

Some deviations in the spectrum from an ideal blackbody distribution are visible. These spectral features are remaining

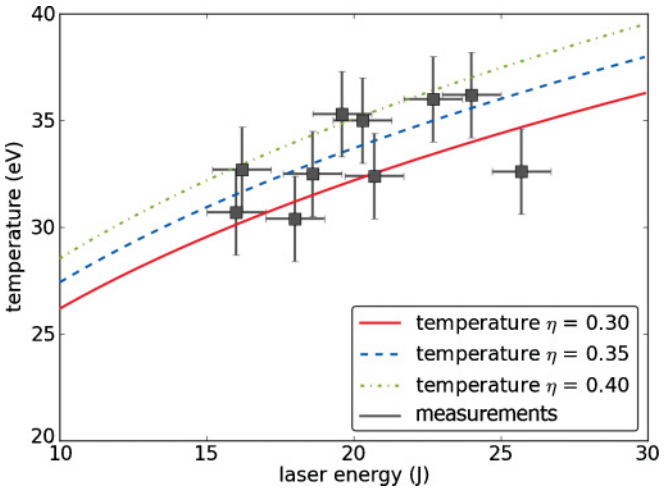

FIG. 6. (Color online) Measured and calculated temperatures using the scaling law from Eq. (3) with varying conversion efficiencies from laser energy to primary x rays η. All cavities were spherical and had a diameter of 750 μm.

characteristics of the gold plasma, in particular, transitions to the O shell. This is to be expected since neither gold nor any other material is perfectly opaque to this energetic thermal radiation [21].

VII. DISCUSSION

In these experiments the radiation temperature of laser-heated hohlraum targets was successfully determined with two independent diagnostics. From the time-resolved measurements the brightness temperature as well as the temperature evolution during the heating with the laser was resolved and maximum values of 35 eV were measured. The influence of time integration on spectral measurements with regular spectrometers to determine the radiation temperature were found to be minimal; integrated measurements were in very good agreement to maximum temperatures measured with the diode spectrometer. A comparison of the scaling law [Eq. (3)] with experimental data gives an excellent agreement for conversion efficiencies η of laser energy to primary x rays of 30%–40%. The influence of the losses through holes is small because $f \approx 0.06$ for our cavities. One main reason for the fluctuation of the data is expected to be small variations of the laser alignment from the center of the small cavity entrance hole. The low-energy wings of the heating laser are sufficient to produce plasma at the edge of the entrance hole, which prevents a fraction of the laser energy from entering the hohlraum. Calculated and measured temperatures are shown in Fig. 6 for various targets.

A critical factor for indirect heating and energy-loss measurements is the fraction of laser energy that enters the secondary cavity as thermal radiation [see Fig. 1(c)]. The amount of energy transferred into the secondary hohlraum at any point in time is given by the Stefan-Boltzmann law and depends on the temperature and the radiating surface, i.e., one of the holes in the cavity. The total energy must be obtained by integrating over time and this is why the time-resolved diagnostic is crucial to the determination of this efficiency. With a typical diagnostic hole diameter of 150 μm and a measured temperature profile an average of 0.4%–0.5% of the laser energy was emitted as thermal radiation through this hole. In indirect-heating experiments this value clearly has to be optimized. Calculations with a higher temperature and a larger diagnostic hole show that efficiencies of 10% and more can be reached. Future experiments with the PHELIX laser will be able to create temperatures of ~100 eV in the primary and 40 eV in a secondary hohlraum. This will be sufficient to have enough photons in the transparency region near the carbon *K* edge to realize the indirect heating of carbon samples to a relatively cold and dense plasma state for energy-loss experiments.

ACKNOWLEDGMENT

This work was supported in part by BMBF 06DA934 I.

[1] J. Lindl, Phys. Plasmas **2**, 3933 (1995).
[2] R. Sigel, Plasma Phys. Control. Fusion **29**, 1261 (1987).
[3] Th. Löwer, R. Sigel, K. Eidmann, I. B. Földes, S. Hüller, J. Massen, G. D. Tsakiris, S. Witkowski, W. Preuss, H. Nishimura, H. Shiraga, Y. Kato, S. Nakai, and T. Endo, Phys. Rev. Lett. **72**, 3186 (1994).
[4] A. Benuzzi, Th. Löwer, M. Koenig, B. Faral, D. Batani, D. Beretta, C. Danson, and D. Pepler, Phys. Rev. E **54**, 2162 (1996).
[5] D. Batani, T. Desai, Th. Löwer, T. A. Hall, W. Nazarov, M. Koenig, and A. Benuzzi-Mounaix, Phys. Rev. E **65**, 066404 (2002).
[6] R. L. Kauffman, L. J. Suter, C. B. Darrow, J. D. Kilkenny, H. N. Kornblum, D. S. Montgomery, D. W. Phillion, M. D. Rosen, A. R. Theissen, R. J. Wallace, and F. Ze, Phys. Rev. Lett. **73**, 2320 (1994).
[7] S. H. Glenzer, L. J. Suter, R. E. Turner, B. J. MacGowan, K. G. Estabrook, M. A. Blain, S. N. Dixit, B. A. Hammel, R. L. Kauffman, R. K. Kirkwood, O. L. Landen, M.-C. Monteil, J. D. Moody, T. J. Orzechowski, D. M. Pennington, G. F. Stone, and T. L. Weiland, Phys. Rev. Lett. **80**, 2845 (1998).
[8] I. B. Földes, K. Eidmann, G. Veres, J. S. Bakos, and K. Witte, Phys. Rev. E **64**, 016410 (2001).
[9] M. Tabak, J. Hammer, M. E. Glinsky, W. L. Kruer, S. C. Wilks, J. Woodworth, E. M. Campbell, M. D. Perry, and R. J. Mason, Phys. Plasmas **1**, 1626 (1994).
[10] M. Roth, T. E. Cowan, M. H. Key, S. P. Hatchett, C. Brown, W. Fountain, J. Johnson, D. M. Pennington, R. A. Snavely, S. C. Wilks, K. Yasuike, H. Ruhl, F. Pegoraro, S. V. Bulanov, E. M. Campbell, M. D. Perry, and H. Powell, Phys. Rev. Lett. **86**, 436 (2001).
[11] A. Frank, A. Blažević, P. L. Grande, K. Harres, T. Heßling, D. H. H. Hoffmann, R. Knobloch-Maas, P. G. Kuznetsov, F. Nürnberg, A. Pelka, G. Schaumann, G. Schiwietz, A. Schökel,

M. Schollmeier, D. Schumacher, J. Schütrumpf, V. V. Vatulin, O. A. Vinokurov, and M. Roth, Phys. Rev. E **81**, 026401 (2010).
[12] M. M. Basko, J. Maruhn, and An. Tauschwitz, J. Comput. Phys. **228**, 2175 (2009).
[13] I. Sofronov *et al.*, Trudy VNIIEF **1**, 25 (2001).
[14] R. Pakula and R. Siegel, Phys. Fluids **28**, 232 (1984).
[15] R. E. Marshak, Phys. Fluids **1**, 24 (1958).
[16] R. Sigel, R. Pakula, S. Sakabe, and G. D. Tsakiris, Phys. Rev. A **38**, 5779 (1988).
[17] J. Shao-En, Sun Ke-Xu, Ding Yong-Kun, Huang Tian-Xuan, Cui Yan-Li, and Chen Jiu-Sen, Chin. Phys. Lett. **22**, 2328 (2005).
[18] G. Schaumann, M. S. Schollmeier, G. Rodriguez-Prieto, A. Blažević, E. Brambrink, M. Geissel, S. Korostiy, P. Pirzadeh, M. Roth, F. B. Rosmej, A. Ya. Faenov, T. A. Pikuz, K. Tsigutkin, Y. Maron, N. A. Tahir, and D. H. H. Hoffmann, Laser Part. Beams **23**, 503 (2005).
[19] K. Witte, V. Bagnoud, A. Blazevic, S. Borneis, C. Bruske, J. Caird, S. Calderon, D. Eimerl, U. Eisenbarth, J. Fils, R. Fuchs, S. Götte, T. Hahn, G. Klappich, F. Knobloch, T. Kühl, S. Kunzer, M. Kreutz, R. Lotz, T. Merz-Mantwill, E. Onkels, D. Reemts, M. Roth, A. Roussel, T. Stöhlker, A. Tauschwitz, R. Thiel, U. Thiemer, B. Zielbauer, and D. Zimmer, GSI Scientific Report, 2008 (unpublished).
[20] A. Ben-Kish, A. Fisher, E. Cheifetz, and J. L. Schwob, Rev. Sci. Instrum. **71**, 2651 (2000).
[21] T. J. Orzechowski, M. D. Rosen, H. N. Kornblum, J. L. Porter, L. J. Suter, A. R. Thiessen, and R. J. Wallace, Phys. Rev. Lett. **77**, 3545 (1996).